IEEE Access
Multidisciplinary ⋮ Rapid Review ⋮ Open Access Journal

Received October 18, 2020, accepted November 11, 2020, date of publication November 19, 2020,
date of current version December 8, 2020.

Digital Object Identifier 10.1109/ACCESS.2020.3039423

Rework the Radio Link Budget for 5G and Beyond

KAMIL BECHTA[1], JINFENG DU[2], (Member, IEEE), AND MARCIN RYBAKOWSKI[1]
[1]Mobile Networks, Nokia, 54-130 Wrocław, Poland
[2]Bell Labs, Nokia, Holmdel, NJ 07733, USA

Corresponding author: Kamil Bechta (kamil.bechta@nokia.com)

ABSTRACT The 5th generation of mobile communication system (5G) enables the use of millimeter wave frequency bands and beamforming with narrow-beam directional antennas for mobile communication. Accurate estimation of radio link budget which enables direct assessment of achievable cell range or maximum throughput and facilitates network parametrization before deployment is one of the most challenging problems in radio network planning. In contrast to traditional cellular systems, where omni-directional or sectoral antennas are deployed with half-power beam-width much larger than angular spread of the radio channel, the beam-width of antenna arrays assumed for 5G in sub-6GHz and millimeter wave bands can be comparable to or smaller than channel angular spread in scattering environment. Since the effective antenna pattern is determined jointly by the nominal antenna pattern and channel angular spread, it is no longer appropriate to use nominal pattern in radio link budget analysis or system level simulations. Simplified approach, where nominal pattern is assumed for all typical propagation conditions, results in overestimation of the signal power in serving links and underestimation of interference, which in consequence gives erroneous estimation of link budget and leads to unsatisfactory network design and deployment. To avoid inaccurate calculation of link budget while maintaining simplicity it is proposed to modify the simplified approach by using effective antenna patterns. On the other hand, effective antenna pattern can be further optimized by matching its half-power beam-width to the angular spread of the radio channel. It is demonstrated via simulations how to rework the radio link budget for accurate estimation of system performance in high bands for 5G and beyond, along with benefits of effective antenna pattern optimization.

INDEX TERMS 5G, angular spread, beamforming, directional antenna, effective antenna pattern, millimeter wave, radio link budget.

I. INTRODUCTION

The first wave of commercial deployment of the 5th generation of mobile communication system (5G) started in early 2019. The 5G New Radio (NR) [1], which was named by 3rd Generation Partnership Project (3GPP) - a standardization body - to emphasize its revolutionary nature, can deliver up to Gbps download data rate in selected locations, which is over ten times higher than what 4G (Long Term Evolution - LTE) [2] can provide. However, we have already learned that the performance of these first networks is not always as expected by the end users, and coverage has been a big challenge from day one. What are the most common reasons of the first 5G networks unsatisfactory performance?

One of the answers is overestimation of radio link budget. Overestimation in this case means that at the stage of network planning the assumed coverage of the cell and the level of downlink (DL) signal power from serving base station (BS) were higher than what was measured in the field. As a consequence, the DL signal to interference plus noise ratio (SINR), and therefore DL throughput, are lower than initially expected.

As different as reasons of SINR overestimation can be, the most probable one is too simplified method of link budget calculation, inherited from previous generations of cellular system analysis. In traditional cellular systems where omni-directional or sectoral antennas are deployed, the antenna half-power beam-widths (HPBW) are much larger than angular spread of the radio channels. Therefore, the impact of channel angular spread on link budget is negligible and the simplified method works. However, 5G NR is adapted to use - in both sub-6GHz and millimeter waves (mmWave) bands - antenna arrays whose beam-width is comparable to or smaller than channel angular spread. The complex relation

The associate editor coordinating the review of this manuscript and approving it for publication was Hassan Tariq Chattha.

between 5G narrow-beam directional antennas and channel angular spread should be carefully examined and properly accounted for in 5G radio link budget calculation. Inheriting the simplified radio link budget tool from previous generations would lead to noticeable difference in SINR as compared to detailed simulation results using three-dimensional (3D) channel modeling. Inaccurate estimation of SINR *"may lead to suboptimal deployments of first 5G networks"*, a direct quote from [3].

This article summarizes the authors' latest studies on proper modeling of 5G link budget with narrow-beam antennas and its impact on network performance estimation. Section II introduces definitions of nominal and effective antenna beam patterns. In Section III two different methods for simple link budget calculation are presented and their estimation of 5G network performance is compared. Section IV shows the efficiency of antenna tapering from the perspective of effective antenna beam pattern. A method for optimization of effective antenna beam pattern is provided in Section V, and system level simulation results are presented in Section VI. Section VII summarizes and concludes the article.

II. NOMINAL ANTENNA PATTERN VS. EFFECTIVE ANTENNA PATTERN

When designing an antenna, one of the main objectives is to obtain a specific radiation pattern. In case of antenna arrays, the expectations are mostly high maximum gain and low level of side lobes. Antenna pattern which has been determined by design and validated by measurements in an anechoic chamber is referred to hereinafter as *nominal antenna pattern* of the antenna.

With increasing number of antenna elements in the array, the maximum gain of the nominal antenna array pattern increases and its HPBW decreases. These relations are described by [4]:

$$g^{Nom}_{\max} = \frac{2}{B_{ho} \cdot B_{vo}} = N \cdot G_e, \tag{1}$$

where $g^{Nom}_{\max}$ is the maximum nominal antenna array gain, B_{ho} and B_{vo} are the nominal root mean square (RMS) beam-width in horizontal and vertical planes (in radians), respectively, N is the number of antenna elements in the array, and G_e is the gain of a single antenna element.

In practical channel scattering environment, which differs significantly from anechoic chamber propagation conditions, the maximum realizable gain and associated HPBW of an antenna array differ from their nominal values and are hereinafter referred to as effective. Therefore, the antenna pattern measured in a scattering environment is defined as *effective antenna pattern* for that channel.

Nominal antenna pattern and nominal gain are antenna specific, whereas effective antenna patterns and the corresponding effective gains change depending on a channel. The difference between nominal and effective antenna patterns depends on an angular spread in the scattering environment introduced by a real deployment scenario. Equations (2)-(4) describe how effective antenna patterns can be analytically obtained based on nominal antenna pattern and power angular spectrum (PAS) of the assumed propagation environment.

$$g^{Eff}(\phi_0, \theta_0) = \int_{-180^\circ}^{180^\circ} \int_{0^\circ}^{180^\circ} g^{Nom}(\phi, \theta) \cdot p(\phi - \phi_0, \theta - \theta_0)\, d\phi d\theta, \tag{2}$$

$$g^{Eff}_{Az}(\phi_0) = g^{Eff}(\phi_0, \theta_0 = 90^\circ) = \int_{-180^\circ}^{180^\circ} g^{Nom}(\phi, \theta = 90^\circ) \cdot p_{Az}(\phi - \phi_0) d\phi, \tag{3}$$

$$g^{Eff}_{Ele}(\theta_0) = g^{Eff}(\phi_0 = 0^\circ, \theta_0) = \int_{0^\circ}^{180^\circ} g^{Nom}(\phi = 0^\circ, \theta) \cdot p_{Ele}(\theta - \theta_0) d\theta. \tag{4}$$

In the above equations g^{Eff} is the 3D effective antenna pattern, whereas g^{Nom} is the 3D nominal antenna pattern. g^{Eff}_{Az} and g^{Eff}_{Ele} indicate azimuth and elevation cuts of effective antenna pattern, respectively. ϕ and θ define angular domain in azimuth and elevation, respectively, whereas ϕ_0 and θ_0 indicate boresight direction between transmitter (Tx) and receiver (Rx) in azimuth and elevation, respectively. p_{Az} and p_{Ele} represent realizations of PAS in azimuth and elevation, respectively.

The level of antenna gain degradation, defined as a difference between nominal and effective antenna gain, depends on propagation environment of antenna deployment. Series of measurement campaigns of effective antenna pattern in different deployment scenarios have been performed and published in [5]–[8]. For instance, Fig. 1 presents samples of measurement results performed in a factory propagation environment [7]. The polar plot presented indicates how effectively the shape of directional antenna pattern can vary between consecutive measurements, even in the line of sight (LOS) conditions. Despite of very strong direct path, the multipath propagation components impact the outcome effective pattern noticeably. As can be expected, nominal pattern is degraded even more significantly in case of non-line of sight (NLOS) conditions, where the direct path is not present, and outcome effective pattern is formed only by multipath components. It is visible that NLOS effective beam pattern is wider than in LOS case and its main direction in horizontal plane is less obvious as there are many clusters with similar strength in measured radio channel.

Fig. 2 presents a summary of statistically analyzed measurement results in different deployment scenarios, i.e. indoor office [5], suburban fixed wireless access (FWA) [6], factory automation [7] and urban Manhattan street canyons [8]. In all the scenarios a severe impact of angular spread on effective antenna gain is visible. In case of NLOS the reduction in

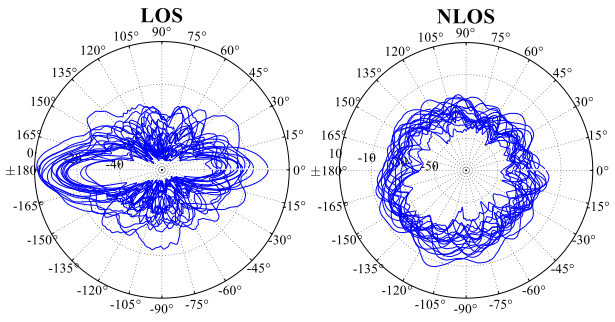

FIGURE 1. Horizontal angular spectra of effective directional antenna patterns measured in indoor factory environment [7].

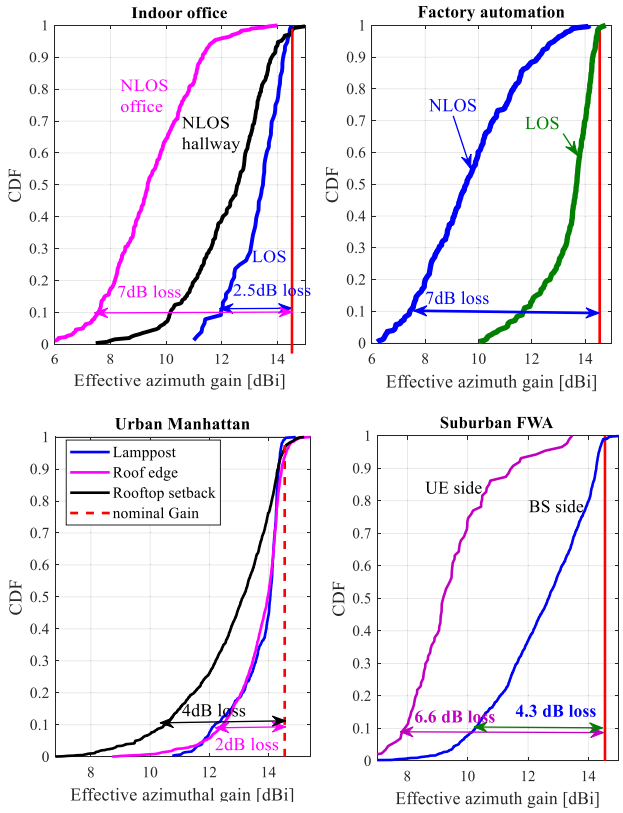

FIGURE 2. CDFs of effective antenna gains measured in indoor office [5], suburban FWA [6], factory automation [7] and urban Manhattan [8] environments presented in comparison with nominal antenna gain.

azimuth gain can be as high as 7 dB for 10% of measured radio links or 5 dB for 50% of measured radio links, in reference to maximum nominal gain of 14.5 dBi in azimuth.

Those measurement results demonstrate that nominal antenna patterns, as measured in an anechoic chamber, are valid only in free space propagation conditions. This conclusion is particularly important in the context of simulation campaigns which were aimed to estimate performance of 5G system before the commercial deployment began. Reliable simulation results should have ensured correctness of minimum requirements for 5G equipment and helped to better optimize the first 5G networks deployed in the field.

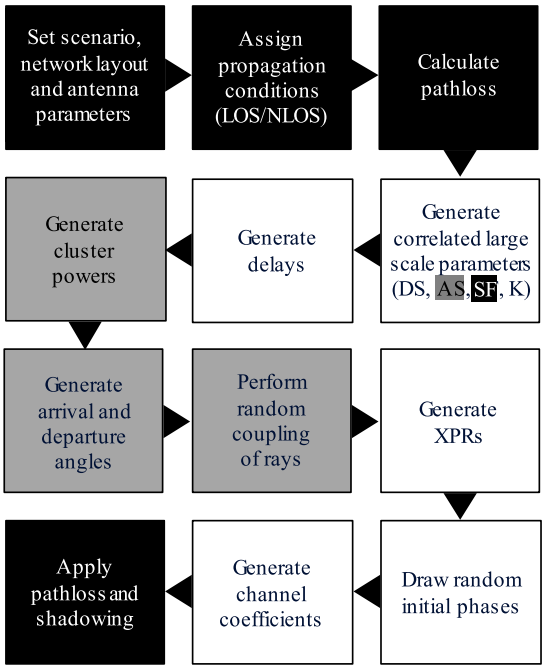

FIGURE 3. Block diagram of statistical channel model reconstruction according to 3GPP [9].

We already know that it was not always the case. Next section demonstrates how the performance estimated for typical deployment scenarios can deviate from realistic values if in link budget calculations the nominal antenna pattern is wrongly used instead of realistic effective pattern.

III. RADIO LINK BUDGET: HOW IT SHOULD BE DONE?

For link-level and detailed system-level simulations, 3GPP [9] has provided instruction on how to generate statistical 3D channel models, as shown in Fig. 3, which includes all the necessary radio propagation phenomena that must be taken into account during comprehensive simulation to provide estimation of radio link budget and performance.

However, such detailed simulation is very time- and resource-consuming, and could be prohibitively complex, especially for system level simulation with many radio links needed to be calculated for evaluation of useful and interference signals conditions. To meet a growing need for quick link budget estimation and system performance evaluation, a simplified method, which considers only the black blocks from Fig. 3, is commonly used, for example in [10] for coexistence studies.

According to section 5.2.5 of [10] the model of received power in DL and uplink (UL) should include only path loss and directional antenna gains, determined based on nominal antenna patterns taken from antenna datasheet. Such an approach considers only some of large-scale parameters of a radio channel model, i.e. path loss and shadowing, but neglects other relevant parameters, especially angular spread, which determines effective antenna pattern. Therefore, the real impact of angular spread on the effective antenna

gain is lost in the link budget calculation, which leads to inaccurate estimation of received power.

The simplified method was popular in evaluations of previous generations wireless networks as the antenna beam-width is usually much larger than the channel angular spread, and the difference between nominal and effective antenna gain is small. 5G, however, adopts much narrower antenna beam-width and the gap between nominal and effective antenna gain is too large to be ignored, as evidenced by the measurement results presented in Section II (which clearly show that angular spread leads to a decrease of nominal antenna gain).

Therefore, to avoid inaccurate calculation of link budget while maintaining simplicity, it is proposed to use only black blocks from Fig. 3 but on top of that apply the effective antenna patterns defined by (2), instead of nominal antenna patterns, according to the following steps:

1. Determine the nominal antenna pattern applicable for a given radio link (as in the simplified approach).
2. Determine the PAS.
3. Calculate 3D effective antenna pattern according to (2) based on nominal antenna pattern and PAS as determined in Step 1 and Step 2.
4. Determine the effective antenna gain applicable for evaluated radio link based on the geometry determined by the positions of Tx and Rx and effective antenna pattern from Step 3.

The above method can be used in case of analog beamforming or panel-based hybrid beamforming where the beamforming vector can be drawn from Grid of Beams (GoB) codebook, conventional Fourier transform based beamforming, or other advanced beamforming techniques such as eigen beamforming and zero forcing beamforming.

PAS in Step 2 can be constructed either on a per-scenario basis, i.e. one PAS for all links in the same deployment scenario, or on a per-user equipment (UE) basis with one unique PAS for each UE. The former has negligibly increased complexity, and the per-scenario PAS can be derived based on the statistical channel model applicable for assumed propagation scenario (e.g. by realization of gray blocks from Fig. 3 for model [9]) or from the angular spread measurements performed in the analyzed environment (e.g. [6]). For illustration, Fig. 4 presents the nominal and effective antenna patterns of an 8 × 8 BS antenna array at 28 GHz with per-scenario PAS for the UMi SC deployment scenario [11]. Noticeable difference between nominal and effective patterns, especially in case of NLOS conditions and side lobes, would translate directly into DL SINR values.

The per-UE PAS generation can be done in the similar way as the per-scenario case but requires UE-specific angular spread and cluster realization. This will bring desired accuracy at the cost of slightly increased complexity.

In Fig. 5 a comparison is made of the CDFs of DL SINR for the UMi SC deployment scenario [11] using four methods: 1) a simplified approach with nominal patterns; 2) a simplified approach with effective patterns generated by per-scenario PAS; 3) a simplified approach with effective patterns generated by per-UE PAS; 4) a full-scale 3D simulation.

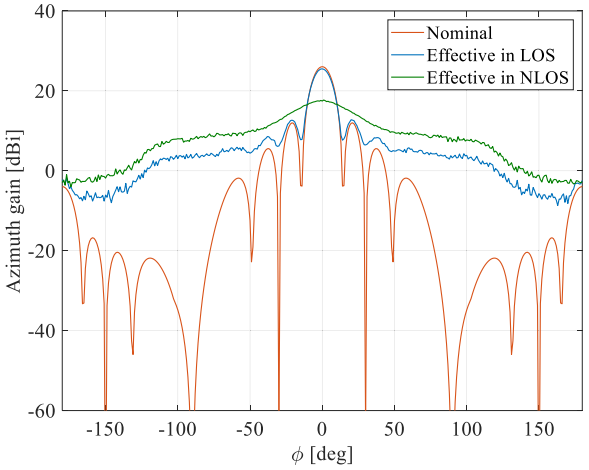

FIGURE 4. Nominal and effective Tx antenna pattern cuts in horizontal plane for 8 × 8 array in mmWave (28 GHz) 3GPP UMi SC deployment [11].

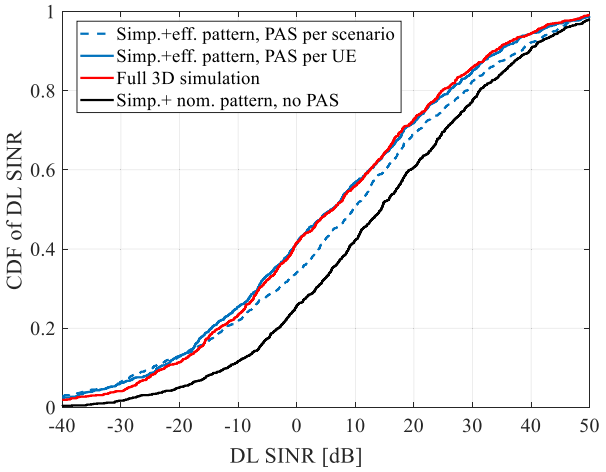

FIGURE 5. CDFs of DL SINR for mmWave 3GPP UMi SC deployment scenario [11] (combined LOS and NLOS links).

Compared to the complex and time-consuming full-scale 3D simulation (treated as ground truth for 3GPP related studies), the results obtained by simplified method with nominal pattern can be over 10 dB too optimistic at 10^{th} percentile and over 8 dB at median. The CDF of simplified approach with effective patterns generated by per-UE PAS is within 1 dB from the ground truth for a wide range of percentiles (from 10^{th} to 99^{th}). When per-scenario PAS is used, the accuracy decreases slightly (2 dB gap at 10^{th} percentile and 3 dB gap at median). Therefore, using effective patterns can provide significantly more accurate results - closer to full 3D simulation results - than those obtained for nominal pattern. In the rest of this paper per-UE PAS will be used when using effective patterns because of its excellent accuracy with marginal added complexity.

To demonstrate the significance of using effective antenna pattern in system level simulations of 5G networks a comparison is made of the results obtained using nominal antenna patterns as suggested in 3GPP [10] against the results obtained using effective antenna patterns (with per-UE PAS), for deployment scenarios of urban macro (UMa) and urban micro street canyon (UMi SC) [11] as well as suburban FWA [12]. The focus is put on the cumulative distribution function (CDF) curves for DL SINR obtained in system level simulations with Monte Carlo methodology for stochastic channel model [9] using the simplified method, for both nominal and effective antenna patterns.

DL Rx power from serving link (DL S) or from an inter-cell interfering link (DL I) are calculated as:

$$P_{Rx} = \frac{P_{Tx} \cdot G_{Tx} \cdot G_{Rx}}{PL}, \tag{5}$$

where P_{Rx} and P_{Tx} are Rx and Tx power respectively, whereas G_{Rx} and G_{Tx} are Rx and Tx antenna gains used for calculation of a given radio link. PL indicates path loss. For link i, either for a serving link or interfering link, the Tx (Rx) antenna gains were determined by Gn^i_{Tx} (Gn^i_{Rx}) or Ge^i_{Tx} (Ge^i_{Rx}) for nominal or effective antenna patterns, respectively. These gains are presented by (6)-(9).

$$Gn^i_{Tx} = g^{Nom}_{Tx}\left(\phi^{AoD}_{i,LOS} - \phi^{AoD}_{i,BF}, \theta^{ZoD}_{i,LOS} - \theta^{ZoD}_{i,BF}\right), \tag{6}$$

$$Gn^i_{Rx} = g^{Nom}_{Rx}\left(\phi^{AoA}_{i,LOS} - \phi^{AoA}_{i,BF}, \theta^{ZoA}_{i,LOS} - \theta^{ZoA}_{i,BF}\right), \tag{7}$$

$$\begin{aligned} Ge^i_{Tx} &= \sum_{j=1}^{N_i} Gn^{i,j}_{Tx} \cdot P_{i,j} \\ &= g^{Eff}_{Tx}\left(\phi^{AoD}_{i,LOS} - \phi^{AoD}_{i,BF}, \theta^{ZoD}_{i,LOS} - \theta^{ZoD}_{i,BF}\right), \end{aligned} \tag{8}$$

$$\begin{aligned} Ge^i_{Rx} &= \sum_{j=1}^{N_i} Gn^{i,j}_{Rx} \cdot P_{i,j} \\ &= g^{Eff}_{Rx}\left(\phi^{AoA}_{i,LOS} - \phi^{AoA}_{i,BF}, \theta^{ZoA}_{i,LOS} - \theta^{ZoA}_{i,BF}\right). \end{aligned} \tag{9}$$

In (6)-(9) $g_{Tx}(\phi^{AoD}, \theta^{ZoD})$ and $g_{Rx}(\phi^{AoA}, \theta^{ZoA})$ are the 3D nominal/effective patterns of Tx and Rx antennas, respectively. $\phi^{AoD}_{i,LOS}$, $\theta^{ZoD}_{i,LOS}$, $\phi^{AoA}_{i,LOS}$ and $\theta^{ZoA}_{i,LOS}$ represent angles of LOS direction between Tx and Rx in azimuth and elevation for radio link i. $\phi^{AoD}_{i,BF}$, $\theta^{ZoD}_{i,BF}$, $\phi^{AoA}_{i,BF}$ and $\theta^{ZoA}_{i,BF}$ represents directions in azimuth and elevation for which main beams of Tx and Rx antennas are pointed (beamformed). In (8) and (9), $Gn^{i,j}_{Tx}$ and $Gn^{i,j}_{Rx}$ indicate nominal gains of transmitting and receiving antennas respectively for multipath j of radio link i. $P_{i,j}$ is the power carried by multipath j ($j = 1, 2, \ldots, N_i$) of radio link i and $\sum_{j=1}^{N_i} P_{i,j} = 1$.

TABLE 1 summarizes differences in simulation results obtained by application of nominal and effective patterns. Due to the presence of a strong directive path in LOS condition, the effective antenna gain is close to nominal gain, whereas in NLOS conditions the effective gain is noticeably lower. This difference in the gains causes the overestimation of the DL S using the nominal pattern. On the other hand, angular spread of radiated energy in horizontal plane causes increased effective gain of side lobes as compared to the nominal values in both LOS and NLOS conditions. This is the reason of underestimation of DL I by calculations with nominal pattern, because the major part of interference is received by the side lobes. Therefore, the use of nominal pattern causes overestimation of DL S and underestimation of DL I, which leads to significantly overestimated DL SINR in all simulated deployment scenarios, as large as 14 dB for UMi SC. These results clearly show that a simplified method with nominal pattern for 5G network estimation can give an erroneous picture of performance metrics which cannot be met in real field deployments.

TABLE 1. Summary of 5G 28 GHz networks performance obtained from system level simulation results for different deployment scenarios [11], [12].

Deployment scenario	UMa [11]		UMi SC [11]		FWA [12]
	LOS	**NLOS**	**LOS**	**NLOS**	**Vegetation LOS**
Array size of BS	16x16		8x8		8x8
Nominal gain [dBi]	32.0		26.0		24.0
Effective gain [dBi]	31.5	21.0	25.5	17.5	20.0
Nominal median *DL S* [dBm]	-19.5	-31.0	-51.7	-61.3	-63.1
Effective median *DL S* [dBm]	-21.4	-45.6	-54.3	-74.7	-68.4
Nominal median *DL I* [dBm]	-57.6		-72.7		-102.6
Effective median *DL I* [dBm]	-53.2		-66.9		-95.5
Nominal median *DL SINR* [dB]	**30.2**		**14.2**		**12.7**
Effective median *DL SINR* [dB]	**16.4**		**4.4**		**7.4**

IV. EFFICIENCY OF ANTENNA ARRAY TAPERING IN REAL PROPAGATION ENVIRONMENT

Previous sections clearly demonstrated that effective antenna pattern may be significantly different from nominal antenna pattern, which has been proved by simulations and measurements. Impact on the main lobe is visible especially in NLOS conditions, whereas substantial increase in the level of side lobes is observed for both LOS and NLOS conditions. The difference between the main lobe gain and the first side lobe gain, commonly referred as the first sidelobe suppression level (SSL), is usually around 13 dB for square antenna arrays without amplitude tapering. In practice, this difference can be further increased by an application of tapering [13] (attenuation of amplitude of outer antenna elements in the array) at the cost of loss in nominal gain of the main lobe. Application of tapering, as one of the common approaches in 5G to suppress side lobe level, helps to decrease the energy

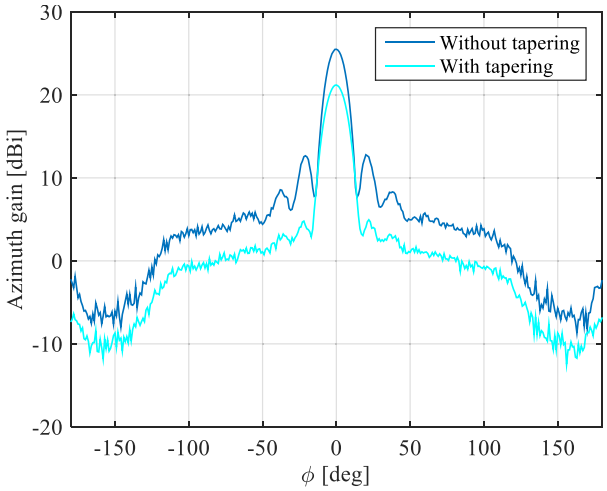

FIGURE 6. Effective Tx antenna pattern cut in horizontal plane for 8 × 8 array in mmWave 3GPP UMi SC deployment for LOS conditions [14].

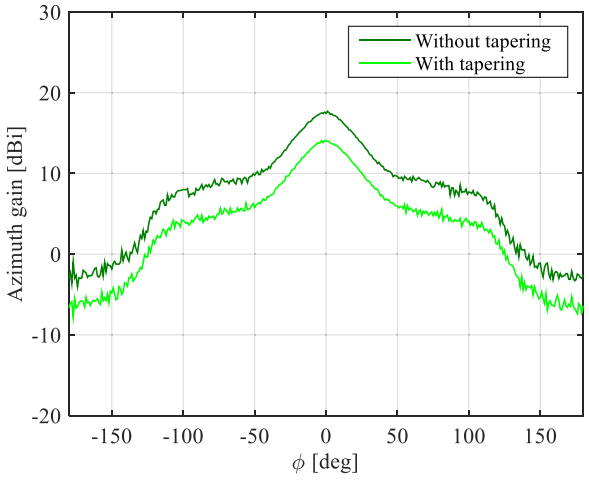

FIGURE 7. Effective Tx antenna pattern cut in horizontal plane for 8 × 8 array in mmWave 3GPP UMi SC deployment for NLOS conditions [14].

radiated/captured to/from undesired directions and therefore minimize the power of interference in the radio channel.

However, if angular spread in scattering environment impacts the shape of nominal antenna pattern, for which tapering is applied, what is the impact on tapering efficiency?

To address this question, a system level simulation was performed for UMa and UMi SC scenarios with 16 × 16 and 8 × 8 antenna arrays, respectively [14]. Tapering was applied by multiplication of uniform magnitudes of antenna array beam weight factors by coefficients obtained from Chebyshev function [15] to minimize the bandwidth or smearing while forcing all side lobes to be below a specified level, which in this study was set to 20 dB. For nominal pattern the obtained SSL is 20.6 dB for 16 × 16 array and 21.5 dB for 8 × 8 array, in line with the design of the Chebyshev tapering window.

In LOS conditions, as shown in Fig. 6 for UMi SC with 8 × 8 array, the drop in gain of the main lobe is lower than the drop in gain of the first side lobe, and therefore the tapering still helps to improve the system's SINR. However, the reduction of tapering effectiveness even in LOS, with effective SSL of 16.3 dB in contrast to the nominal 21.5 dB SSL without angular spread, should be considered during network deployment, where the interference from side lobes is crucial for performance evaluation.

In NLOS conditions, as shown in Fig. 7, the same level of gain drop is observed for the main lobe and side lobes, which suggests that tapering is not an efficient method in NLOS conditions with the effective SSL as low as 3.4 dB. Similar observations apply to the 16 × 16 array under UMa channels [14].

For 5G networks, where tapering is used, it is therefore important to verify whether the design of the antenna array with applied tapering is validated under realistic propagation conditions.

V. METHOD FOR ANTENNA ARRAY OPTIMIZATION

Directional antenna performs spatial filtering of electromagnetic energy from the space, and it is reasonable to match the antenna pattern to the PAS of the channel in given propagation conditions. In [16] a detailed solution was presented of how to maximize the energy radiated to or captured from the space for a given array size and channel angular spread constraints. It has been verified by laboratory and field measurements for determination of the optimal antenna array geometry for uniform planar arrays with analog beamforming. For convenience, the fundamentals of the solution from [16] are quoted below.

It was assumed that N antenna elements, arranged in rectangular/square shape, form a uniform planar array of size $(K_1; K_2)$, with:

$$K_1 K_2 \leq N. \tag{10}$$

The array of $(K_1; K_2) = (1; N)$ corresponds to a horizontally deployed uniform linear array, whereas $K_2 = 1$ indicates a vertically deployed uniform linear array. Let B_{ve} and B_{he} be the nominal beam-widths of the antenna elements whose gain is G_e. The nominal RMS beam-widths B_{v0} and B_{h0} of the analog beams formed by antenna array of size $(K_1; K_2)$ can be approximately described as:

$$B_{v0} = \frac{B_{ve}}{K_1}, \quad B_{h0} = \frac{B_{he}}{K_2}. \tag{11}$$

The effective beamforming gain can be determined based on nominal antenna pattern and channel angular spread [4] as:

$$G\left(N, B_{ve}, B_{he}, \sigma_v, \sigma_h\right) = \frac{2}{\sqrt{\left(\frac{B_{ve}}{K_1}\right)^2 + \sigma_v^2}\sqrt{\left(\frac{B_{he}}{K_2}\right)^2 + \sigma_h^2}}, \tag{12}$$

where σ_h and σ_v are the RMS azimuth spread of departure (ASD) and RMS zenith spread of departure (ZSD), respectively.

Since the effective gain (12) depends on the panel geometry $(K_1; K_2)$, and B_{ve} and B_{he} are determined by the antenna

element via $G_e = 2/(B_{ve}B_{he})$, the array geometry $(K_1; K_2)$ can be optimized to maximize the effective beamforming gain G stated in (12) subject to the size constraint (10). While ignoring the integer constraint on array dimension K_1 and K_2, the effective beamforming gain is maximized if and only if the array geometry is given by:

$$K_1 = \sqrt{\frac{NB_{ve}\sigma_h}{B_{he}\sigma_e}}, \quad K_2 = \sqrt{\frac{NB_{he}\sigma_v}{B_{ve}\sigma_h}}. \tag{13}$$

The nearest integer pair close to $(K_1; K_2)$ as specified by (13) and satisfying the total elements constraint (10) gives the best analog beamforming gain and constitutes the *optimal antenna array pattern*. Next section demonstrates the efficiency of the method presented and its impact on improvement of performance in a 5G network.

VI. FROM ANTENNA ARRAY OPTIMIZATION TO IMPROVED LINK BUDGET

System level simulation results of improved single-user (SU) MIMO performance of mmWave 5G FWA small cells network deployed in a suburban area were presented in [12]. By optimizing antenna array configuration from 8×8 to 16×4 for a given channel angular spread, the DL SINR has been improved by 2 dB, which led to the increase of DL cell capacity by 60% at the cell edge.

However, some concerns may be raised regarding the impact of antenna pattern widening in horizontal plane (due to optimization) on interference in multi-user (MU) scenario. Therefore, this section includes new simulation results to quantify the impact of antenna array optimization on DL performance in MU-MIMO scenario. The focus is put on the DL signal strength S, interference to noise ratio (INR), SINR and throughput. For each of the above metrics the results for antenna arrays of size 64 and 144 elements are presented with 2 or 4 simultaneously served UE per cell.

A. SIMULATION ASSUMPTIONS

As 3GPP in [9] does not define channel model for suburban environment, the simulation study presented in this section is based on 3GPP UMi SC stochastic model improved by statistics obtained for suburban 28 GHz measurement campaign presented in [6]. No site-specific channel characteristic was assumed. TABLE 2 includes the main angular spread characteristics of channel model, which are used to estimate the effective beam patterns for link budget calculation.

For system level simulations a suburban area of approximate dimension 700 m $\times$ 600 m was assumed, which consisted of 16 blocks. Each block contained 20 houses, 10 per each side of the same street, and was served by 2-sectoral BS. Fig. 8 illustrates detailed topology of modelled FWA network. It was assumed that 10% of houses which are the closest to BSs have indoor Customer Premise Equipment (CPE), whereas for the remaining 90% of houses outdoor CPE was assumed. For path loss calculation the empirical models presented in [6], [17] and summarized in TABLE 3 were used.

TABLE 2. Angular spread model assumed for system study of 5G FWA in suburban area at 28 GHz (azimuth spread of departure, ASD; zenith spread of departure, ZSD; azimuth spread of arrival, ASA; zenith spread of arrival, ZSA).

Propagation condition	$\log_{10}$ (ASD/1°)	$\log_{10}$ (ZSD/1°)	$\log_{10}$ (ASA/1°)	$\log_{10}$ (ZSA/1°)
LOS	$\mu = 1.14$ $\sigma = 0.41$ [9]	$\mu = 0.15$ $\sigma = 0.35$ [9]	$\mu = 1.21$ $\sigma = 0.12$ [6]	$\mu = 0.58$ $\sigma = 0.28$ [9]
VLOS	$\mu = 0.82$ $\sigma = 0.24$ [6]	$\mu = 0.05$ $\sigma = 0.35$ [9]	$\mu = 1.21$ $\sigma = 0.12$ [6]	$\mu = 0.86$ $\sigma = 0.31$ [9]
NLOS	$\mu = 0.82$ $\sigma = 0.24$ [6]	$\mu = 0.05$ $\sigma = 0.35$ [9]	$\mu = 1.21$ $\sigma = 0.12$ [6]	$\mu = 0.86$ $\sigma = 0.31$ [9]

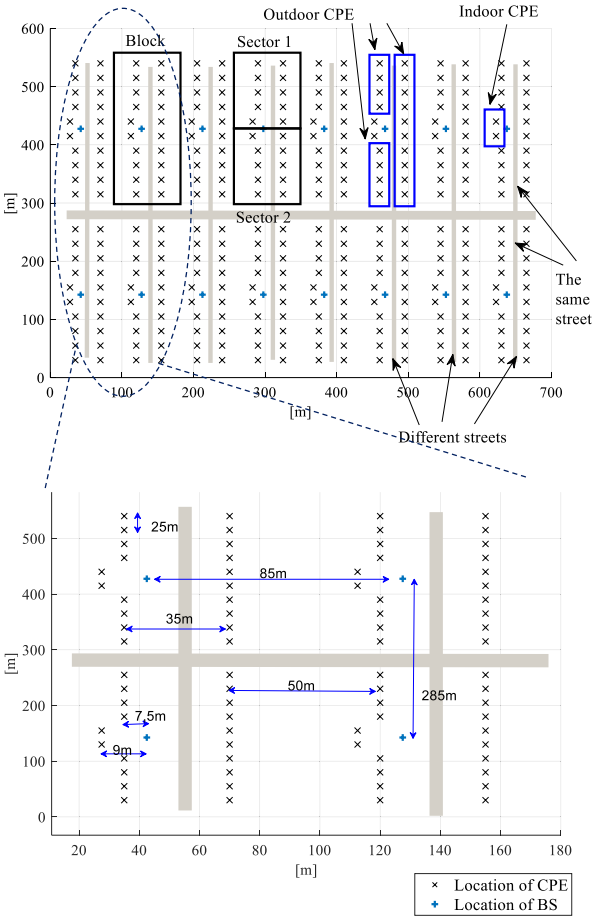

FIGURE 8. Topology of a mmWave FWA network in suburban area.

Vegetation LOS conditions (VLOS) were assumed for wanted signal links towards outdoor CPE and for interfering links from other sectors but placed on the same street. LOS path loss model with additional Outdoor-to-Indoor (O2I) penetration loss [17] was assumed for serving links towards indoor CPE. Thus, VLOS conditions applied to 90% of all simulated wanted signal links, whereas the remaining 10% stayed in LOS conditions with additional O2I loss. NLOS

TABLE 3. Assumed path loss model for suburban area [6].

Propagation conditions	Path loss [dB] (d [m]: 2D distance between BS and CPE)	Shadow fading [dB]
LOS	$61.4 + 24.0 \cdot \log_{10}(d)$	4.2
VLOS	$45.1 + 40.6 \cdot \log_{10}(d)$	6.4
NLOS	$80.3 + 31.3 \cdot \log_{10}(d)$	4.8
O2I loss	Mean 15.1 dB, standard deviation 2.5 dB [17]	

TABLE 4. Main assumptions of system level simulations for estimation of the performance in mmWave 5G FWA network in suburban environment.

BS	
Carrier frequency	28 GHz
Channel bandwidth per UE	800 MHz
Antenna array pattern (nominal)	According to [18]
Gain of single antenna element	6 dBi
Antenna array configuration (M * V × H)	For N=64: M*8x8 and M*16x4; For N=144: M*12x12 and M*24x6; M={2,4}
Max total Tx power per polarization (without losses)	28 dBm
Height of antenna array centre	8 m
CPE	
Number of simultaneously served CPEs	{2,4} / sector
Antenna array pattern (nominal)	According to [18]
Gain of single antenna element	6 dBi
Antenna array configuration (V × H)	1 antenna element
Height of antenna centre	1.5 m
Orientation in horizontal plane	Towards BS
Orientation in vertical plane	Towards BS
Rx NF	9 dB

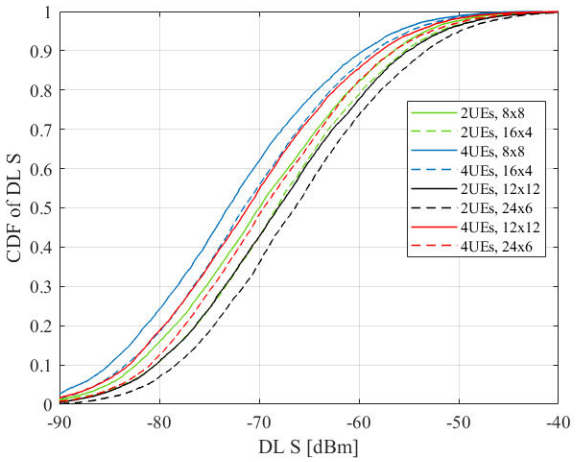

FIGURE 9. CDFs of DL S per UE for mmWave suburban FWA deployment with MU-MIMO (combined LOS and NLOS links).

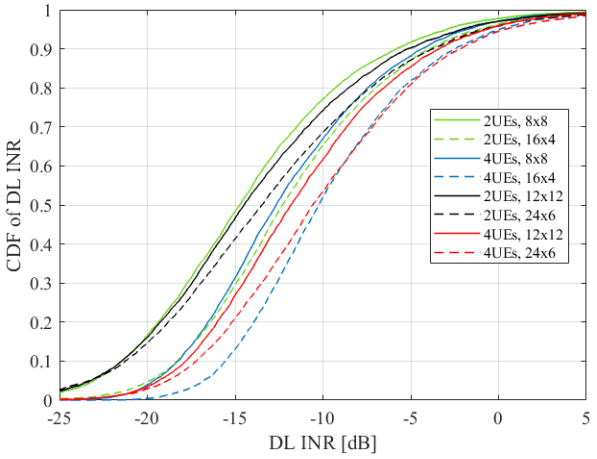

FIGURE 10. CDFs of DL INR per UE for mmWave suburban FWA deployment with MU-MIMO (combined LOS and NLOS links).

conditions were assumed in case of interfering links from BSs placed on a different street than the street where victim CPE was placed. Interfering link from the same cell (intra-cell interference) followed the same condition as wanted signal link. Other predefined suburban FWA deployment parameters, as shown in TABLE 4, are chosen judiciously to represent a realistic deployment scenario.

B. SIMULATION RESULTS

Simulation results have been obtained from system level simulations using Monte Carlo methodology, following the 3GPP stochastic channel model reconstruction as shown in the Fig. 3. Results have been collected in the form of CDFs of the most relevant performance metrics, which provides statistical performance assessment of the FWA network. This approach enables obtaining a broader picture of system performance in reference to deterministic site-specific evaluations. Deterministic channel models, such as clustered delay line (CDL) models of 3GPP [9], are more appropriate for link level simulations and are not in the scope of this work.

Simulation scenario assumes MU-MIMO with analog beamforming per antenna array, which in each sector allows to serve 2 or 4 users at a time. The Maximum Ratio Combining (MRC) precoding has been used for determination of beam pointing directions per polarization.

For the calculation of DL throughput, the model from section 5.2.7 of 3GPP [10] has been used with input SINR obtained from simulations. All the performance metrices are presented for a single stream transmission per user from one polarization of the antenna. In case of MIMO rank 2 the available throughput can be doubled due to high cross-polarization ratio (XPR) in most of the radio channels [9], which could guarantee low inter-stream interference, even with open loop MIMO precoding schemes.

CDFs of DL S, INR, and SINR are shown in Fig. 9, Fig. 10, and Fig. 11, respectively. Note that optimization of antenna pattern leads to the increase of DL interference by more than

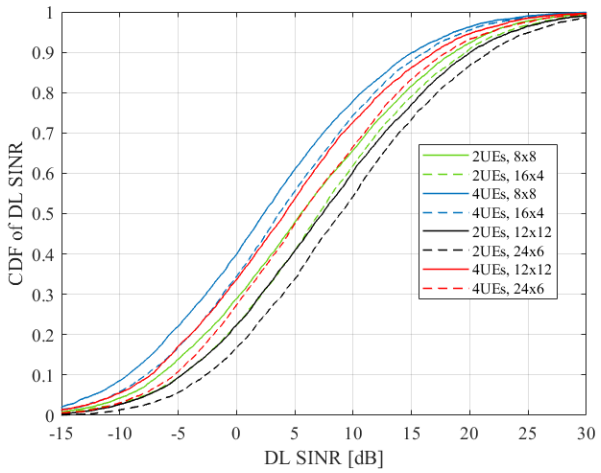

FIGURE 11. CDFs of DL SINR per UE for mmWave suburban FWA deployment with MU-MIMO (combined LOS and NLOS links).

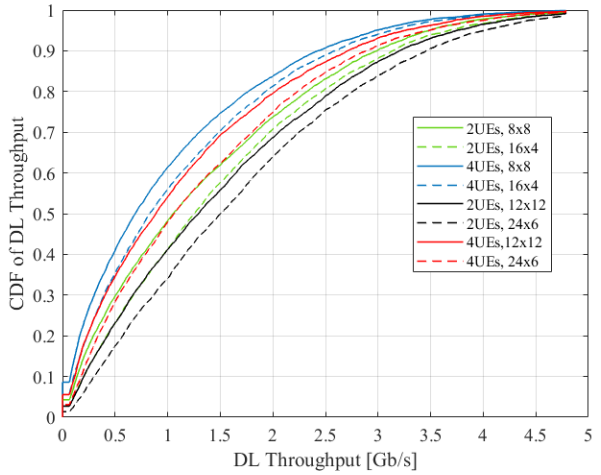

FIGURE 12. CDFs of DL throughput per UE for mmWave suburban FWA with MU-MIMO deployment (combined LOS and NLOS links).

2 dB in median, but due to low INR (95% of links feature interference below the noise level) this rise has negligible impact on DL SINR. The almost 2 dB gain in DL S by optimizing antenna pattern dominates the improvement of DL SINR and throughput (Fig. 12).

TABLE 5 and TABLE 6 contain comparisons of DL SINR and DL throughput for MU-MIMO with 2 and 4 users per cell, when antenna array configurations is optimized from 8×8 to 16×4 and from 12×12 to 24×6, respectively. Optimization of antenna pattern allows 12% to 17% improvement in the DL throughput in median and 39% to 52% improvement at the cell edge. The significant improvement of the cell edge performance is particularly important for mmWave deployments, due to challenging propagation conditions.

VII. CONCLUSION

The deployment of 5G and Beyond networks, which utilize beamforming and mmWave or terahertz (THz), requires careful preparations due to complex relations between narrow-beam directional antenna and challenging propagation

TABLE 5. Summary of system level simulation results of the performance in mmWave 5G FWA network in suburban environment for $N = 64$.

	2UEs, 8x8	2UEs, 16x4	4UEs, 8x8	4UEs, 16x4
DL SINR per UE				
Median	5.5 dB	7.1 dB	2.4 dB	3.6 dB
	→ +1.6 dB →		→ +1.2 dB →	
Cell edge (10%-tile)	-6.6 dB	-4.7 dB	-9.3 dB	-7.8 dB
	→ +1.9 dB →		→ +1.5 dB →	
DL Throughput per UE				
Median	1.1 Gbps	1.3 Gbps	0.8 Gbps	0.9 Gbps
	→ +17 % →		→ +12 % →	
Cell edge (10%-tile)	138 Mbps	200 Mbps	76 Mbps	106 Mbps
	→ +42 % →		→ +39 % →	

TABLE 6. Summary of system level simulation results of the performance in mmWave 5G FWA network in suburban environment for $N = 144$.

	2UEs, 12x12	2UEs, 24x6	4UEs, 12x12	4UEs, 24x6
DL SINR per UE				
Median	7.4 dB	8.9 dB	4.2 dB	5.6 dB
	→ +1.5 dB →		→ +1.4 dB →	
Cell edge (10%-tile)	-4.7 dB	-2.7 dB	-7.4 dB	-5.4 dB
	→ +2.0 dB →		→ +2.0 dB →	
DL Throughput per UE				
Median	1.3 Gbps	1.5 Gbps	0.95 Gbps	1.1 Gbps
	→ +15 % →		→ +16 % →	
Cell edge (10%-tile)	203 Mbps	300 Mbps	116 Mbps	177 Mbps
	→ +48 % →		→ +52 % →	

conditions. When link budget of realistic network is estimated, it is not enough to rely only on nominal antenna pattern, as it occurred in case of omni-directional or sectoral antennas with HPBW much larger than angular spread in the radio channel. In particular, analog beamforming and GoB based hybrid beamforming require effective antenna pattern to be used during estimation of planned network performance and optimization of its parameters. The presented system level simulation results demonstrate that network performance can be overestimated significantly if simplified link budget calculation with nominal antenna pattern is used, which may lead to wrong decisions during network deployments. With a new radio link budget calculation method proposed herein, with slightly added complexity as compared to the simplified approach, the network performance can be estimated accurately and further maximized if optimization of antenna pattern could be done for a given angular spread, leading to about 50% increase of cell edge rate as demonstrated by the FWA example, which is particularly important in challenging propagation conditions of mmWave.

VIII. ACKNOWLEDGMENT

This article was presented in part at the European Conference on Antennas and Propagation 2019 and in part at the 2019 IEEE 5G World Forum.

REFERENCES

[1] *Work Item on New Radio (NR) Access Technology*, document RP-190213, 2019.
[2] *Revised LTE WI Description*, document RP-181726, 2008.
[3] K. Bechta, M. Rybakowski, F. Hsieh, and D. Chizhik, "Modeling of radio link budget with beamforming antennas for evaluation of 5G systems," in *Proc. IEEE 5G World Forum*, Jul. 2018, pp. 427–432.

[4] J. Du, E. Onaran, D. Chizhik, S. Venkatesan, and R. A. Valenzuela, "Gbps user rates using mmWave relayed backhaul with high-gain antennas," *IEEE J. Sel. Areas Commun.*, vol. 35, no. 6, pp. 1363–1372, Jun. 2017.
[5] D. Chizhik, J. Du, R. Feick, M. Rodriguez, G. Castro, and R. A. Valenzuela, "Path loss and directional gain measurements at 28 GHz for non-line-of-sight coverage of indoors with corridors," *IEEE Trans. Antennas Propag.*, vol. 68, no. 6, pp. 4820–4830, Jun. 2020.
[6] J. Du, D. Chizhik, R. Feick, M. Rodriguez, G. Castro, and R. A. Valenzuela, "Suburban fixed wireless access channel measurements and models at 28 GHz for 90% outdoor coverage," *IEEE Trans. Antennas Propag.*, vol. 68, no. 1, pp. 411–420, Jan. 2020.
[7] D. Chizhik, J. Du, R. A. Valenzuela, J. Otterbach, R. Fuchs, and J. Koppenborg, "Path loss and directional gain measurements at 28 GHz for factory automation," in *Proc. IEEE Int. Symp. Antennas Propag. USNC-URSI Radio Sci. Meeting*, Jul. 2019, pp. 2143–2144.
[8] J. Du, D. Chizhik, R. A. Valenzuela, R. Feick, M. Rodriguez, G. Castro, T. Chen, M. Khli, and G. Zussman, "Directional measurements in urban street canyons from macro rooftop sites at 28 GHz for 90% outdoor coverage," *IEEE Trans. Antennas Propag.*, to be published.
[9] *Study on Channel Model for Frequencies From 0.5 to 100 GHz (Release 15)*, document TR 38.901 V15.0.0, 3GPP, 2018.
[10] *Study on New Radio Access Technology; RF and co-existence aspects (Release 14)*, document TR 38.803 V14.0.0, 3GPP, 2018.
[11] K. Bechta, M. Rybakowski, and J. Du, "Impact of effective antenna pattern on millimeter wave system performance in real propagation environment," in *Proc. Eur. Conf. Antennas Propag. (EuCAP)*, 2019, pp. 1–5.
[12] K. Bechta, J. Du, and M. Rybakowski, "Optimized antenna array for improving performance of 5G mmWave fixed wireless access in suburban environment," in *Proc. IEEE 2nd 5G World Forum (5GWF)*, Sep. 2019, pp. 376–381.
[13] C. A. Balanis, *Antenna Theory: Analysis and Design*. Hoboken, NJ, USA: Wiley, 2016.
[14] K. Bechta, M. Rybakowski, and J. Du, "Efficiency of antenna array tapering in real propagation environment of millimeter wave system," in *Proc. Eur. Conf. Antennas Propag. (EuCAP)*, 2019, pp. 1–4.
[15] E. Oran Brigham, *The Fast Fourier Transform and its Applications*. Upper Saddle River, NJ, USA: Prentice-Hall, 1988.
[16] J. Du, M. Rybakowski, K. Bechta, and R. A. Valenzuela, "Matching in the air: Optimal analog beamforming under angular spread," 2019, *arXiv:1910.11054*. [Online]. Available: http://arxiv.org/abs/1910.11054
[17] J. Du, D. Chizhik, R. Feick, G. Castro, M. Rodriguez, and R. A. Valenzuela, "Suburban residential building penetration loss at 28 GHz for fixed wireless access," *IEEE Wireless Commun. Lett.*, vol. 7, no. 6, pp. 890–893, Dec. 2018.
[18] *Radio Frequency (RF) requirement background for Active Antenna System (AAS) Base Station (BS) (Release 13)*, document TR 37.842 V13.0.0, 3GPP, 2016.

KAMIL BECHTA received the M.Sc. degree in wireless communications from the Electronics Faculty, Military University of Technology, Warsaw, Poland, in 2010, where he is currently pursuing the Ph.D. degree in the area of extended modeling of performance and co-existence requirements for 5G and Beyond with massive MIMO antenna configurations.

After graduation, he worked as a Research Assistant with the Military University of Technology, Warsaw, and he joined Nokia Siemens Networks, in 2011, as a 3GPP RAN4 Standardization Specialist responsible for RF and RRM requirements of HSPA and LTE. Since 2015, he has been a 5G Senior Radio Research Engineer with Nokia Bell Labs, where he was leading a team responsible for spectrum and co-existence studies for 5G. In 2017, he was participating in the development of advanced baseband platform software for 5G network products of Nokia, whereas since July 2017, he has been responsible for specification and architecture of radio modules for 5G systems with the Mobile Networks Department, Nokia, Wroclaw. He is a coauthor of more than 15 articles and five patents in the area of wireless communications.

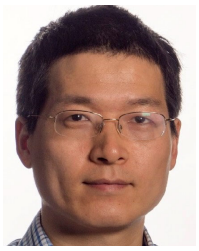

JINFENG DU (Member, IEEE) received the B.Eng. degree in electronic information engineering from the University of Science and Technology of China (USTC), Hefei, China, and the M.Sc., Tekn.Lic., and Ph.D. degrees from the Royal Institute of Technology (KTH), Stockholm, Sweden.

He was a Postdoctoral Researcher with the Massachusetts Institute of Technology (MIT), Cambridge, MA, USA, from 2013 to 2015. After that, he joined Bell Labs, Holmdel, NJ, USA, where he is currently a member of Technical Staff. His research interests include the general area of wireless communications, especially in communication theory, information theory, wireless networks, millimeter wave propagation, and channel modeling.

Dr. Du received the Best Paper Award from IC-WCSP, in October 2010, and his paper was elected as one of the "Best 50 Papers" in the IEEE GLOBECOM 2014. He received the prestigious "Hans Werthen Grant" from the Royal Swedish Academy of Engineering Science (IVA) in 2011, the "Chinese Government Award for Outstanding Self-Financed Students Abroad," in 2012, and the International PostDoc Grant from the Swedish Research Council, in 2013. He also received three grants from the Ericsson Research Foundation.

MARCIN RYBAKOWSKI received the M.Sc. degree in electronics and telecommunication (wireless communication) from the Faculty of Electronics, Wrocław University of Science and Technology, Poland, in 2003, where he is currently pursuing the Ph.D. degree in electromagnetic field exposure for multiantenna systems.

He worked with Becker Avionics, Wroclaw, Poland, as an RF Engineer and Fujitsu, Tokyo, Japan, as an RFIC Engineer. He joined Siemens (then Nokia Siemens Networks), Wroclaw, in 2006, as an Integration and Verification Engineer for 3G and Wimax Base Stations. He has been a Senior Radio Research Engineer with Nokia Solutions and Networks (then Nokia Bell Labs) since 2012, where he was responsible for research on small cells networks for 3G HSPA systems and radio channel modeling for 5G systems. Since 2016, he has been a Senior Specialist at Nokia, and works with the Mobile Networks 5G & Small Cell Architecture Department, Wrocław, where he is responsible for specification and architecture of radio modules for 5G systems. He is the coauthor of more than 15 articles and holds more than ten patents in the area of wireless systems. His research interests include EMF exposure, multiantenna systems, radio wave channel modelling, and evaluation and modelling of wireless systems.

Mr. Rybakowski received the "Young Scientist Award" for the best paper presented at the 10th National Symposium of Radio Science (URSI), and the M.Sc. thesis on microwave, antenna and radar engineering ranked third in a competition organized by the IEEE Polish Section.